Polypyridyl Ruthenium(II) Complexes Functionalized with Fatty Acids for Photodynamic Therapy and Induction of Pyroptosis

Yuan Xu,[a,b] Yatao Hu,[a] Jiaping Cao,[a] Dixin Lin,[a] Qiqi Zhong,[a] Yi Wang,[a*] Hongdong Shi,[c*] Qianling Zhang[a*]

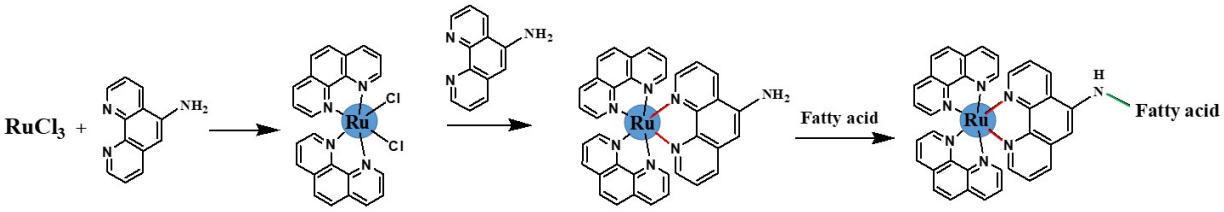

Fig. S1 The synthetic route of the complex $Ru(phen)_2Cl_2(phen\text{-}NH_2)$-Fatty acid (Ru-Cn).

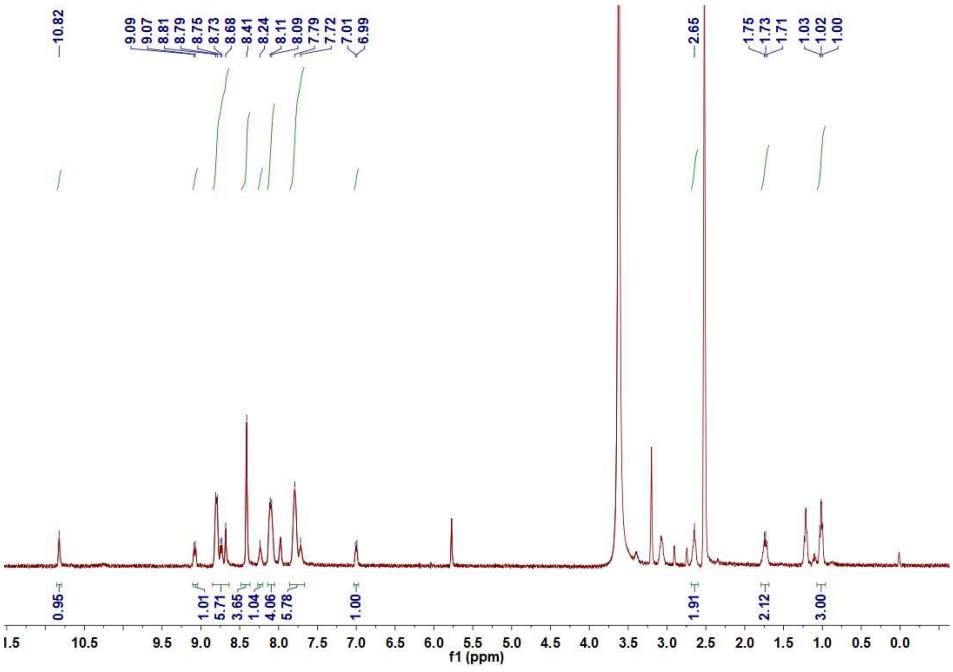

Fig. S2 ^1H NMR spectrum of Ru-C4.

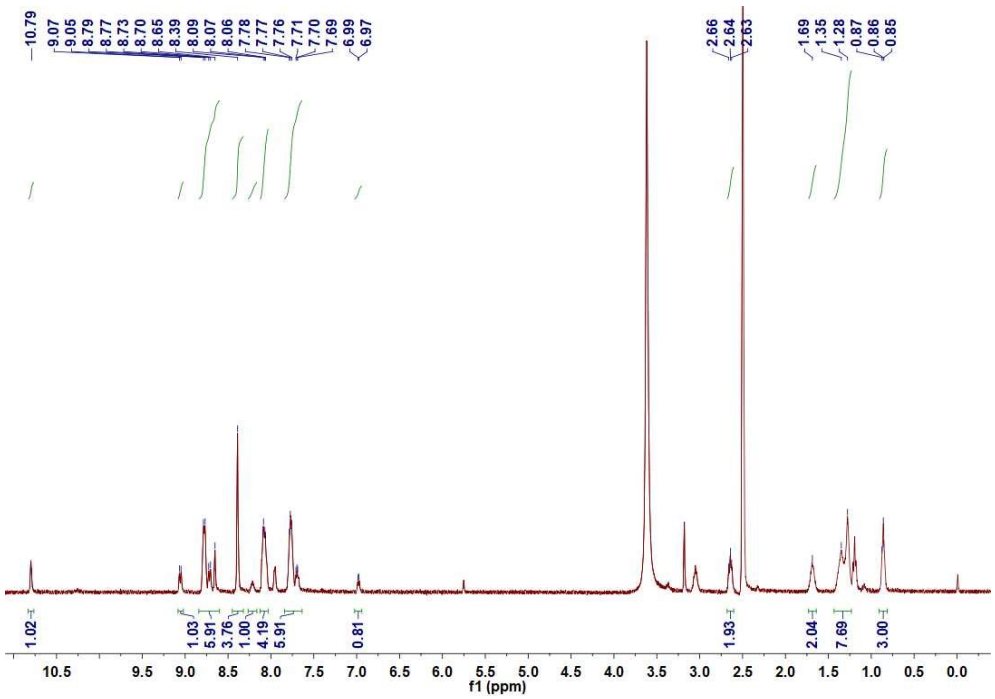

Fig. S3 ^{1}H NMR spectrum of Ru-C8.

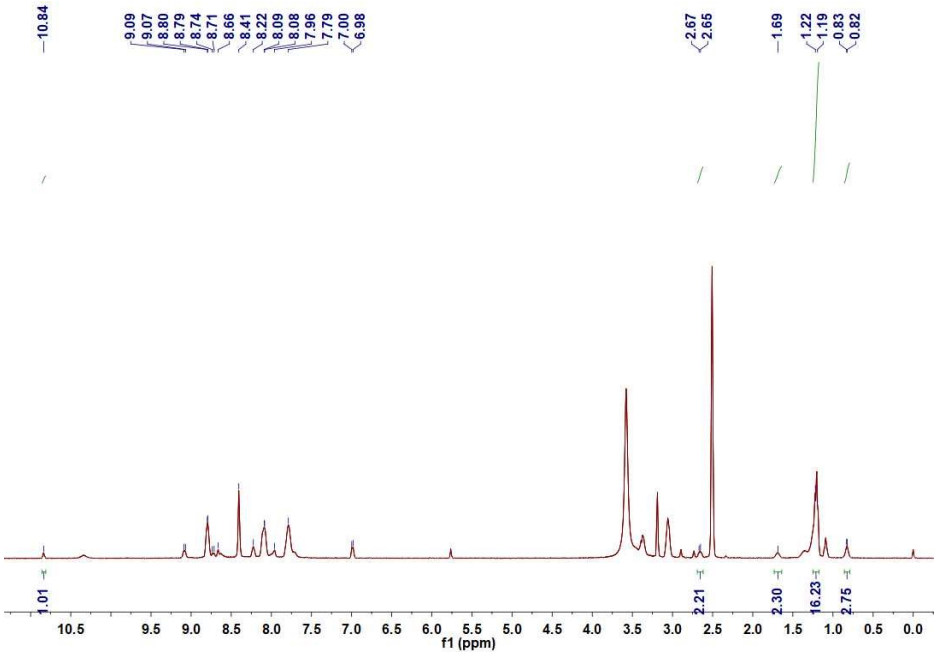

Fig. S4 ^{1}H NMR spectrum of Ru-C12.

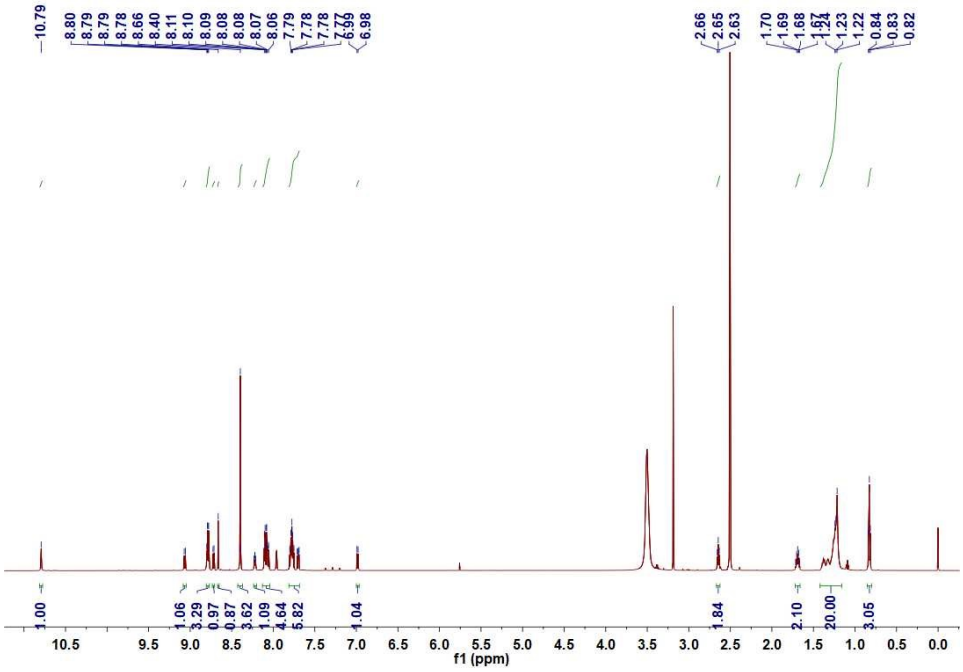

Fig. S5 ^{1}H NMR spectrum of Ru-C14.

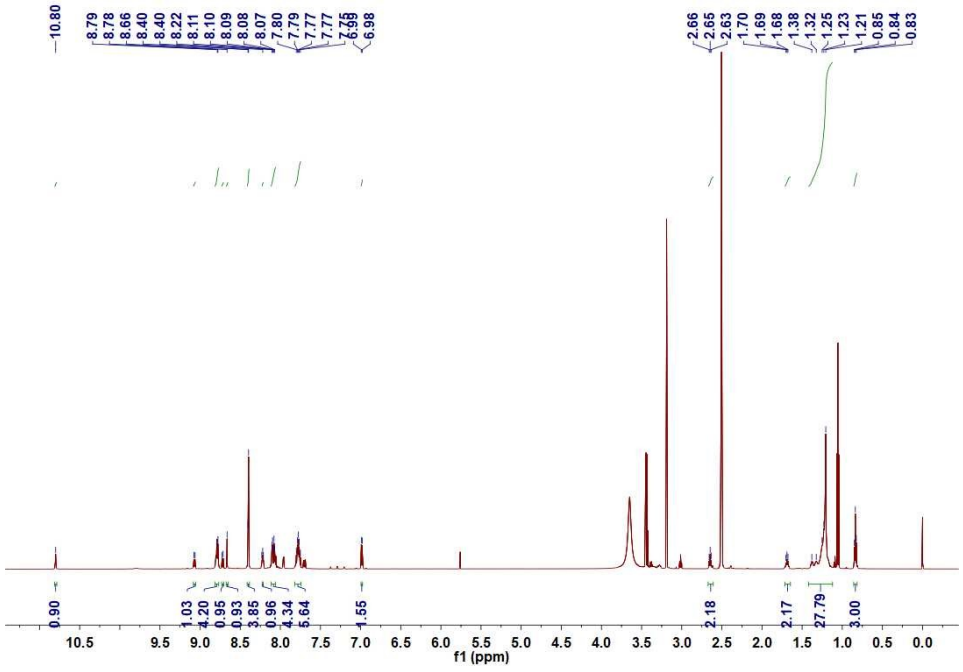

Fig. S6 ^{1}H NMR spectrum of Ru-C18.

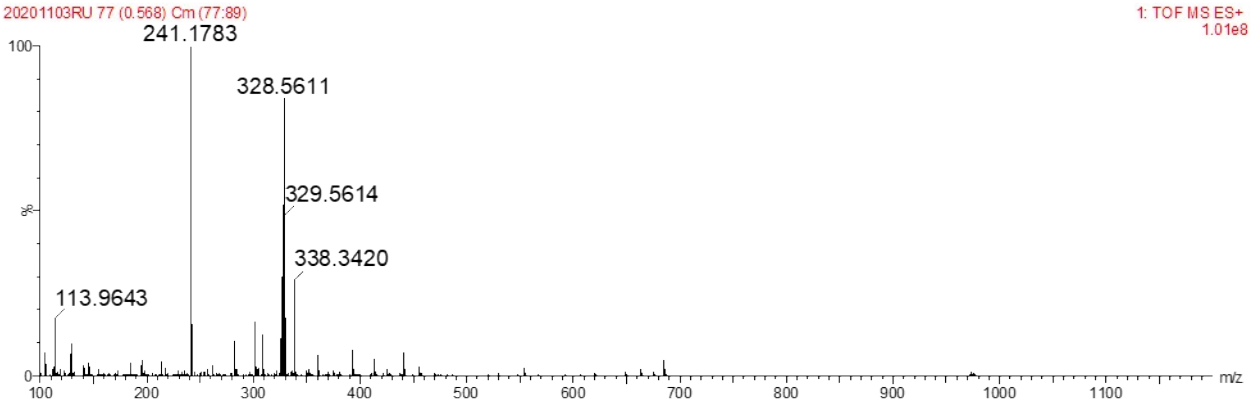

Fig. S7 The ESI-MS spectrum of Ru in CH_3OH.

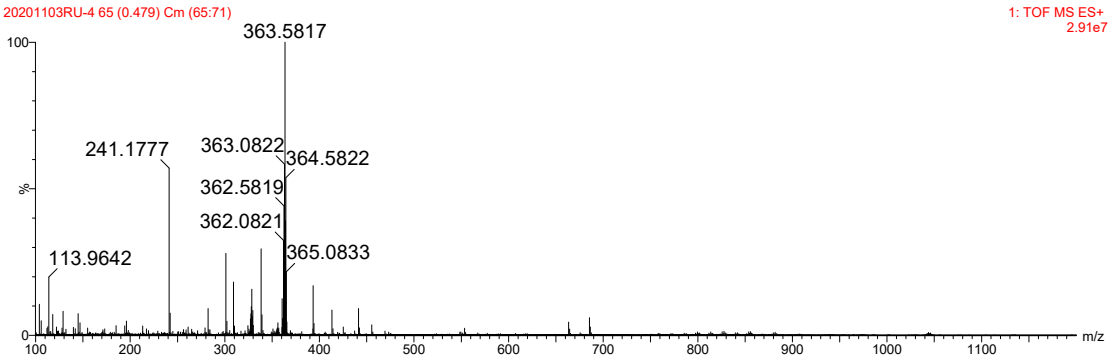

Fig. S8 The ESI-MS spectrum of Ru-C4 in CH_3OH.

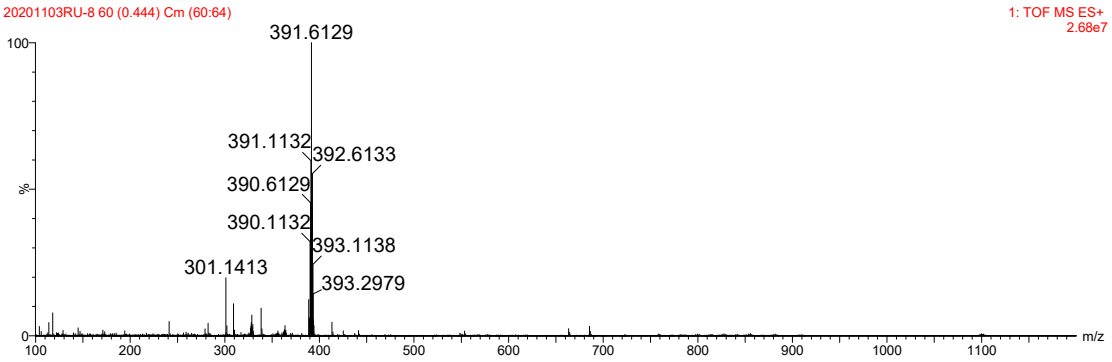

Fig. S9 The ESI-MS spectrum of Ru-C8 in CH_3OH.

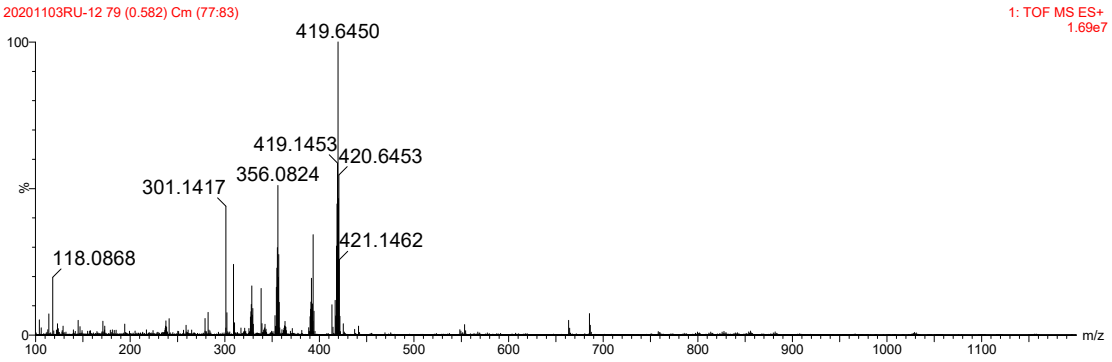

Fig. S10 The ESI-MS spectrum of Ru-C12 in CH_3OH.

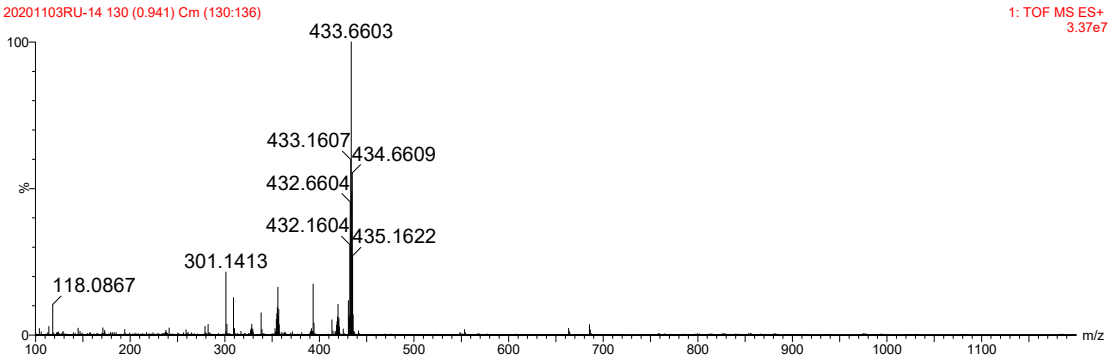

Fig. S11 The ESI-MS spectrum of Ru-C14 in CH_3OH.

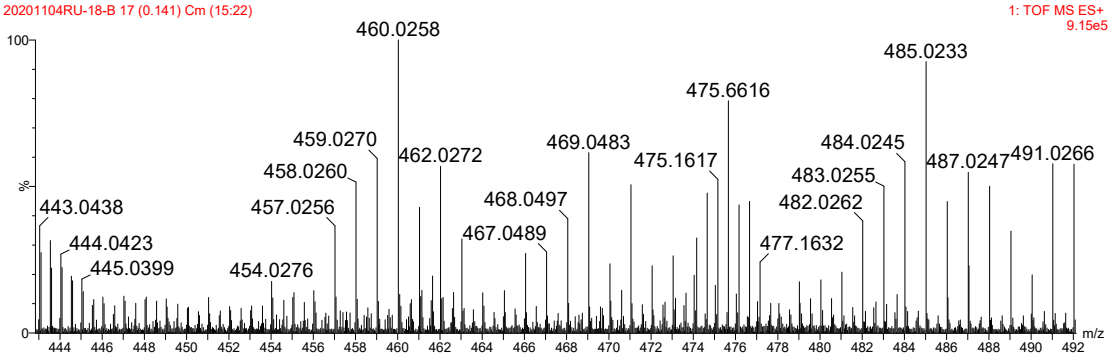

Fig. S12 The ESI-MS spectrum of Ru-C18 in CH_3OH.

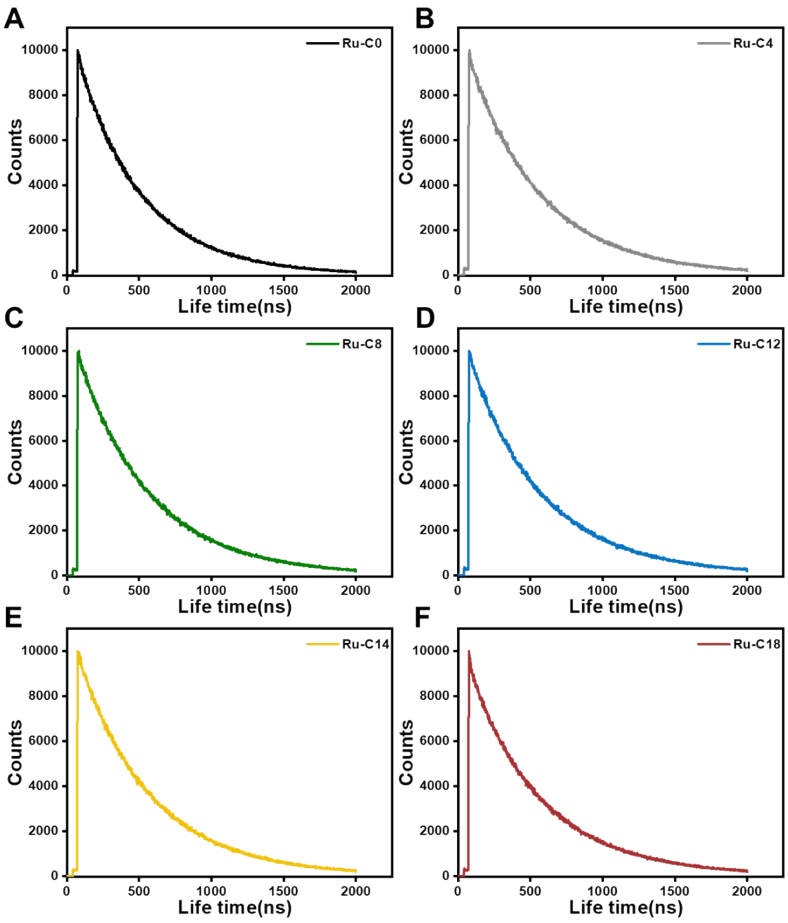

Fig. S13 Fluorescence lifetime decay curves of Ru-Cn complexes.

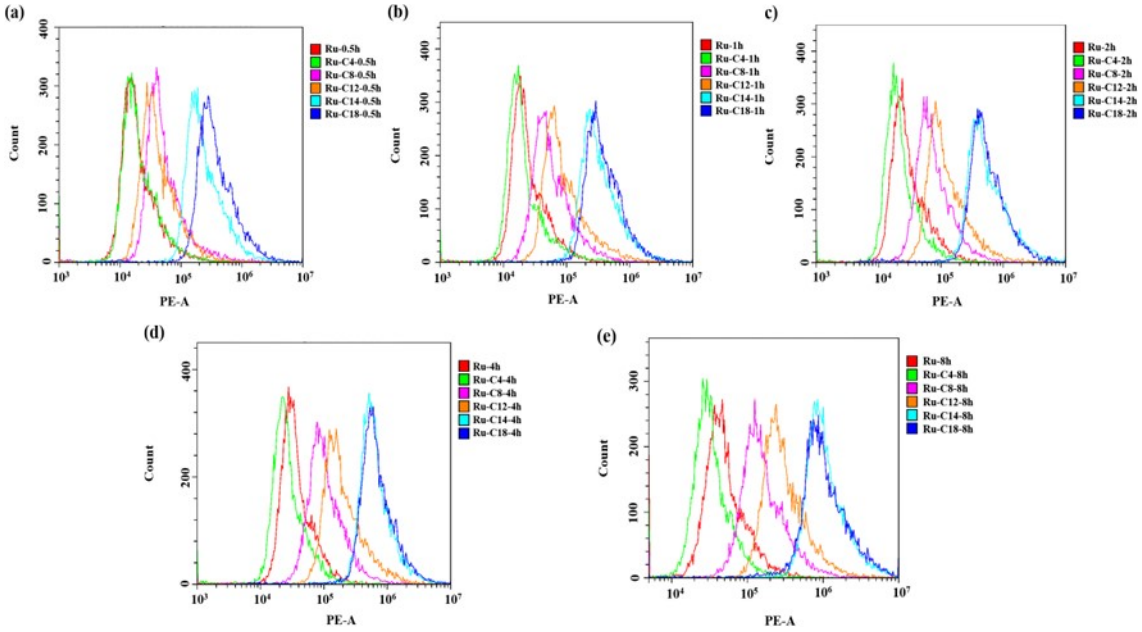

Fig. S14 Flow cytometry analysis of cell uptake of Ru-Cn complexes in Hela cells at different time periods.

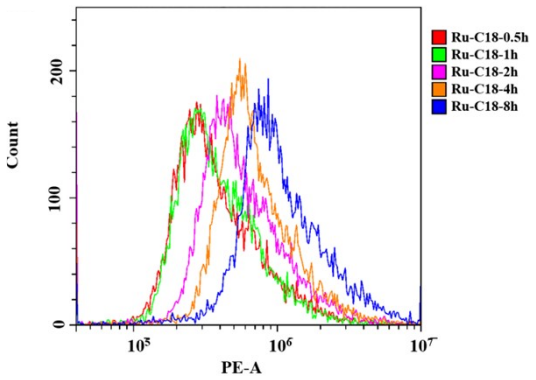

Fig. S15 Flow cytometry analysis of cell uptake of Ru-C18 in HepG-2 cells at different time periods.

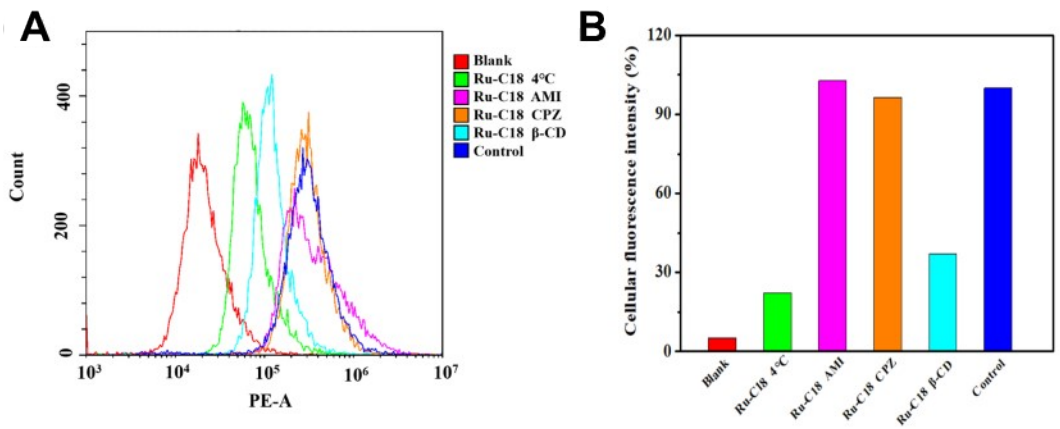

Fig. S16 (A) Cellular uptake of Ru-C18 under different endocytosis inhibition conditions; (B) Summary graph of the mean fluorescence intensity of the detection results.

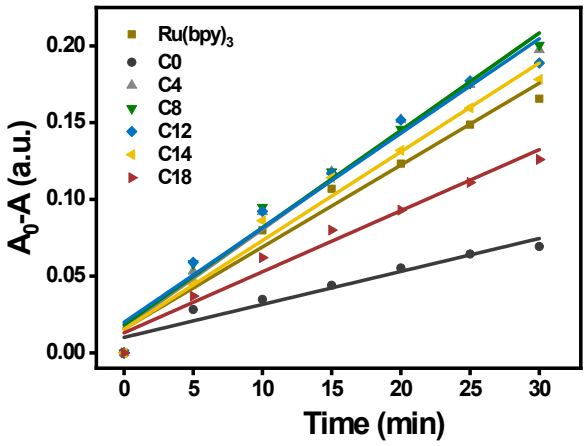

Fig. S17 ROS generation by distinct Ru-Cn complexes under irradiation with 465 nm light (10 mW cm^{-2}).

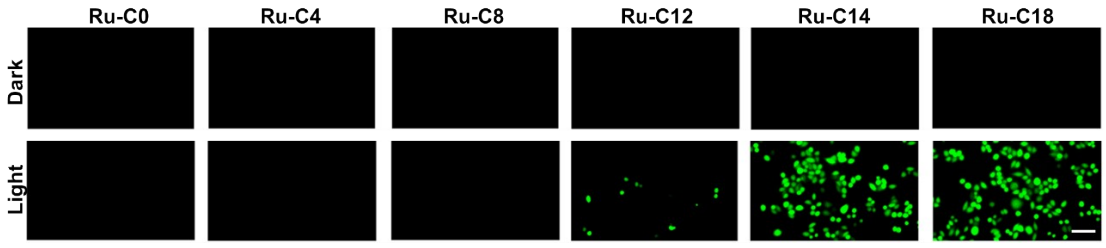

Fig. S18 DCFH-DA was utilized to assess intracellular ROS generation by Ru-Cn complexes following irradiation with 465 nm light (10 mW/cm^2, 30 min, scale bars: 100 μm).

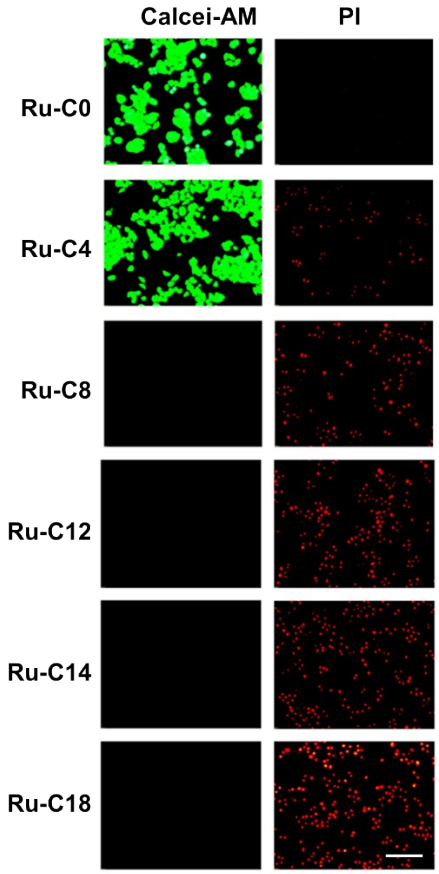

Fig. S19 Fluorescence microscopy images of live and dead cells following treatment with various Ru-Cn complex-based drugs (Scale bars: 100 μm).

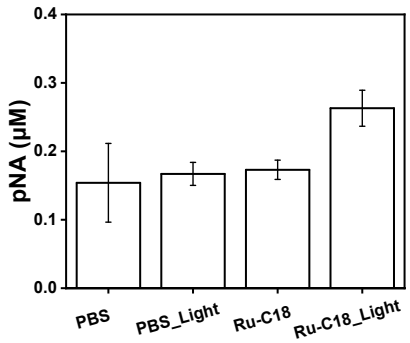

Fig. S20 The Caspase 1 content in cells following co-incubation with Ru-C18 detected by the Caspase 1 Activity Assay Kit.

Table S1 Spectral characterization of a series of Ru-Cn complexes.

Complex	λ_{abs} /nm	λ_{PL} /nm	Φ_{PL}	τ/ns
Ru-C0	448	597	0.45	441.11
Ru-C4	450	599	0.68	497.94
Ru-C8	451	598	0.77	499.52
Ru-C12	450	601	0.76	505.96
Ru-C14	452	600	0.75	500.50
Ru-C18	453	599	0.75	497.13

Table S2 $^1O_2$ generation by a series of Ru-Cn complexes.

Sample	Slope	Φ（$^1O_2$）
$Ru(bpy)_3Cl_2$	0.0054	0.22
Ru	0.0018	0.08
Ru-C4	0.0057	0.24
Ru-C8	0.0056	0.23
Ru-C12	0.0054	O.22
Ru-C14	0.0052	0.22
Ru-C18	0.0035	0.15

Table S3 The cytotoxicity of Ru-Cn complex-based drugs against HepG2 and HeLa cells following incubation for varying durations under 465 nm light irradiation.

IC_{50}/μM		Ru	Ru-C4	Ru-C8	Ru-C12	Ru-C14	Ru-C18
Hep-G2	Dark	＞150	＞150	＞150	＞150	＞50	＞50
	0.5 h	＞150	25.56±2.95	5.26±0.36	1.81±0.16	0.56±0.06	0.51±0.04
	1 h	32.32±3.92	23.99±1.59	2.08±0.15	1.01±0.09	0.55±0.04	0.36±0.02
	2 h	24.82±1.01	14.49±0.97	1.74±0.17	0.84±0.08	0.33±0.03	0.29±0.02
Hela	Dark	＞150	＞150	＞150	＞150	＞50	＞50
	0.5 h	17.78±1.72	12.69±1.03	1.75±0.21	1.38±0.12	0.55±0.04	0.36±0.03
	1 h	14.89±2.11	7.77±0.97	0.87±0.15	0.79±0.13	0.50±0.04	0.34±0.04
	2 h	11.40±1.02	5.51±0.81	0.73±0.14	0.58±0.08	0.29±0.03	0.28±0.02